sustainability

Article

Peak-Load Management of Distribution Network Using Conservation Voltage Reduction and Dynamic Thermal Rating

Ramin Nourollahi [1], Pouya Salyani [1], Kazem Zare [1], Behnam Mohammadi-Ivatloo [1,*] and Zulkurnain Abdul-Malek [2]

[1] Faculty of Electrical and Computer Engineering, University of Tabriz, Tabriz P.O. Box 5166616471, Iran
[2] School of Electrical Engineering, Faculty of Engineering, Universiti Teknologi Malaysia, Johor Bahru 81310, Malaysia
[*] Correspondence: bmohammadi@tabrizu.ac.ir; Tel.: +98-41-3339-3744

Abstract: The peak-load management of a distribution network (DN) has gained attention by increasing the electric power consumption on the demand side. By developing smart-grid infrastructures, effective utilization of the DN's components and proper management of the DN would create a valuable solution for DN operators. Hence, in this paper, a peak-load management framework is proposed in which the real-time rating of the components and voltage-dependent features of the electric loads help the DN operator handle the peak times successfully. In addition to the individual advantages of efficient operation of the DN, more practical results are obtained by combining the conservation voltage reduction (CVR) and dynamic thermal rating (DTR) of the DN's lines and transformers. Based on the obtained results, compared to the individual implementation of CVR, the cost-saving level is increased significantly during the peak events using the simultaneous utilization of DTR and CVR. Furthermore, a discussion is presented about the current problems of the feeders supplying the voltage-dependent constant-power loads during CVR utilization, which is resolved by the dynamic rating of the DN's components.

Keywords: conservation voltage reduction; dynamic thermal rating; distribution network; demand response programs

check for updates

Citation: Nourollahi, R.; Salyani, P.; Zare, K.; Mohammadi-Ivatloo, B.; Abdul-Malek, Z. Peak-Load Management of Distribution Network Using Conservation Voltage Reduction and Dynamic Thermal Rating. *Sustainability* **2022**, *14*, 11569. https://doi.org/10.3390/su141811569

Academic Editor: Enrique Rosales-Asensio

Received: 6 August 2022
Accepted: 8 September 2022
Published: 15 September 2022

1. Introduction

The considerable growth of electric vehicles, distributed generation, and the development of the cities requires efficiently developing communication and control infrastructures to manage the distribution networks (DNs) more efficiently [1]. However, annual load increases and global warming expose the DNs and their equipment to the danger of overloading problems, especially on hot summer days [2]. Privatization of distribution companies, budget limitations, and high costs account for three main obstacles to enhancing equipment capacities by replacement. This issue has obliged the DN owners to optimize existing infrastructure [3] and may lead the DN operator to peak management at the higher loading condition [4]. The developed communication and control infrastructures create an opportunity for the operator to benefit from the advanced DN management system for network management at high loading levels effectively. The developed peak management system includes various items that are important for demand response programs (DRPs) and voltage regulation programs. In addition, to hedge against overheating events, the DN's transformer and line facilities are usually restricted by their thermal limits. In addition to the restriction of line capacity, these thermal limits may lead to some limitations in the voltage regulation of DNs. At the same time, the real-time monitoring of the condition of the systems may help the efficient management of the DN's operation, especially at peak times [5]. Thus, use of the dynamic thermal rating (DTR) instead of conventional rating methods may create opportunities for the DN in effective higher loads level energy management, especially at peak times.

Voltage regulation of the DN is a control strategy to maintain the DN's voltage in a particular range. Depending on the DN's temporary and long-term conditions, voltage regulation plays different roles in the DN by increasing or reducing the voltage [6]. Voltage regulation may be performed for reactive power control or to prevent voltage drop in DN buses at high loading levels. In terms of load management, voltage regulation may be performed as conservative voltage reduction (CVR) to reduce the system's peak load levels and for energy saving [7]. The considerable effects of CVR on reducing energy use and demand levels of DN have been investigated in experimental studies on real distribution feeders [8]. Alongside the technical benefits, the feasibility of economic and engineering benefits of the CVR in the DN's projects has been carried out in [9]. Moreover, the cost–benefit investigation of CVR by introducing an analysis of details of investment return from CVR on the distribution feeders is presented in [10]. In addition to the noted benefits, CVR advantages have been proven in adverse power system problems, such as the power loss reduction that is investigated in [11]. The noted benefits of CVR are related to the demand and energy-saving that happens by voltage reduction in the system. The next application of CVR is in peak load reduction of systems operating near their overheating points [12]. In [7], different methodologies are proposed to quantify CVR's effects at the distribution network's peak times. All the methods proved the significant demand-saving effects of CVR at the peak time, leading to economic benefits.

Changing the line and components (especially transformers) rating method from the conventional static rating to a real-time dynamic rating would increase the DN's nominal current capacity [13]. Some researchers have paid attention to the concept of DTR in DN. Several papers published some thermal models for real-time monitoring of DTR [14]. The International Council initially suggested DTR for the Large Electric Systems Working Group (CIGRE) [15] to increase the line's capacity at significantly lower cost compared to other high-cost methods for expansion planning of the network. The results of an actual project about the DTR established by the Electric Power Research Institute are explained in [16]. As a result of the project, the authors of [16] declare that DTR use increases the transmission line's capacity by about 1–5%. The DTR depends on some weather-based parameters, including wind speed and direction and the ambient temperature, for which the uncertainties of the noted parameters are modeled in [17]. Moreover, in [18], using three types of polynomial regressions, a time-series-based method predicts the power line's DTR values. The DTR has considerable effects on the power line's reliability analysis.

Furthermore, the demand response program (DRP) includes appropriate programs for peak load management in the distribution network [19]. The DRP programs increase resiliency, profitability, and reliability by reducing power consumption at critical times [20]. The customers' load existing in the network is a secure and effective resource available to the network operator to apply the DN's peak load management [21]. In [22], grid operator intervention in the smart grid for residential customers' load to critical peak load management using the customer engagement plans is investigated. The incentive-based interruptable and curtailable DRPs are considered for peak-load management, in which penalizing customers is considered in case of no response to load reduction in order to perform effective peak load management in [23].

Moreover, limited research has coordinated peak load management of CVR, DTR, and DRP methods. In [24], DRP and CVR are coordinated into an advanced DN management system to increase DN efficiency by minimizing the cost of power consumption in the day-ahead market. Furthermore, most of the reviewed DTR literature is related to the transmission network level, whereas very limited research has studied the DTR in DN. In [25], a methodology has been proposed for analyzing the potential advantages of real-time-monitoring-based DTR in the DN from the reliability point of view.

From the reviewed papers, it can be concluded that the CVR application in DN's peak load management solutions has not been appropriately investigated. Moreover, DTR in DN has not been paid adequate attention, especially in the peak load management of DN, which has remained pristine. The authors in this paper aim to address the CVR-based peak management of distribution networks in overloading conditions. On hot summer days, when the network consumption dramatically goes up, the aged distribution networks can face overloading of their substation transformers. Such situations compel the distribution network operator to apply emergency DRPs, which incur an extra high cost to the distribution company. Due to dependence on the market price and penalty cost, the considered emergence load curtailment accounts for DRPs in the distribution system's optimization problems. In addition, this rise in consumption leads to increased power purchasing costs from the upstream network. The CVR is implemented to cope with this problem and reduce the operational and DRP costs so that the minimum cost without any system index violation is attained.

Thus, the contributions of this paper can be summarized as follows:

- This paper addresses the peak management issue through voltage regulation and possible thermal capacity of the network components that, to the best of our knowledge, have not been considered for peak management in the literature.
- CVR method implementation provides the opportunity for peak management at a lower cost than without CVR conditions.
- Considering the thermal rating of distribution network components and their dynamic characteristics, the CVR method with a DTR standpoint releases the components' capacity and reduces the costs of peak management.
- The relevant power flow algorithm based on backward–forward sweep is introduced considering voltage reduction limits and dynamic line rating.

The rest of the paper is organized as follows. Section 2 elaborates on the problem and gives the mathematical formulation. Section 3 discusses the optimization method and the implemented power flow to solve the problem. The proposed method is validated in Section 4, and the ultimate conclusion is presented in Section 5.

2. Problem Formulation

The majority of the studies in the field of DTR have mainly focused on the transmission network of the power system. Because of this, there is no sufficient research on distributed systems. In the same way, this research has come up with a way to determine the DTR of overhead lines in the distribution system, which has not been done properly before because the implementation of DTR in distribution grids needs complicated smart devices. In this paper, a peak-load management framework is proposed for DN. The proposed framework consists of three methods: DTR, DRP, and CVR, with implementation ability in most DNs. Mandatory curtailment is considered the emergent DRP option to lighten the load in the network at critical peak times. This section will introduce the mathematical formulation of the noted methods.

2.1. Conservative Voltage Reduction

It can be safely stated that, in DN, the electrical loads of all feeders depend on the voltage level of the connected bus. In addition, the DN's electrical loads have a different response to the changes in the network voltage. Thus, similar to exponential and ZIP models, various functions are proposed in the literature to model the voltage dependency of DNs' active and reactive loads. In this paper, the ZIP model of voltage dependency is considered to model the active and reactive load changes against voltage regulation. The mathematical formulation of the ZIP model is represented below [26].

$$P_{i,h} = P^0_{i,h}\left[C_{z_p}\left(\frac{V_{i,h}}{V^0_{i,h}}\right)^2 + C_{i_p}\left(\frac{V_{i,h}}{V^0_{i,h}}\right) + C_{p_p}\right] \tag{1}$$

$$Q_{i,h} = Q^0_{i,h}\left[C_{z_q}\left(\frac{V_{i,h}}{V^0_{i,h}}\right)^2 + C_{i_q}\left(\frac{V_{i,h}}{V^0_{i,h}}\right) + C_{p_q}\right] \tag{2}$$

In (1) and (2), $P^0_{i,h}$, $Q^0_{i,h}$, and $V^0_{i,h}$ represent the hourly active, reactive, and voltage of DN buses before implementation of the CVR. In contrast, $P_{i,h}$, $Q_{i,h}$, and $V_{i,h}$, respectively, refer to the hourly active, reactive, and voltage of bus n by voltage reduction. The impacts of voltage reduction on the active power of the DN can be determined through the parameters C_{z_p}, C_{i_p}, C_{p_p} that are the active power constants of ZIP loads. Furthermore, the voltage-dependent behavior of the reactive loads is determined through the constants C_{z_q}, C_{i_q} and C_{p_q}. The voltage dependency of the DN's loads leads to comprehensive changes in the distribution network, from power consumption to current changes, that will be evaluated in the next sections through power flow analysis.

2.2. Dynamic Thermal Rating

The DN's conventional static thermal rating conservatively determines the equipment's rating based on the worst weather conditions, including higher temperatures and the lowest wind speed for overhead lines. The static rating is usually determined separately for each season. Some DN operators may manually change the equipment rating based on their experience and the weather conditions to the practical use of the network capacity. A principled method of developing the smart grid's infrastructure is using DTR to unlock and use the DN capacities. In other words, using the DTR, the DN operator allows more power to be transferred through the network components, which may lead to lesser load curtailment during on-peak times. In order to model the DTR of the DN's different components, IEEE standards [27–29] are used in this paper. The time constants of the components are required in the DTR. The component's time constants depend on the capacitors, and the thermal resistance of these components corresponds to transient responses. The time-constant definition is equal to the required time interval for changing the temperature from the initial temperature (temperature before step change in the load) to 63.2% of the final temperature level (absolute temperature some time after step-change load). The three components of the DN, including transformers, overhead lines, and underground cables, differ in time constants. The thermal time constant related to each of the noted components is roughly equal to 4 h, 15 min, and 8 h for transformers, overhead lines, and underground cables, respectively. A higher time constant leads to lower sensitivity to the short-time changes of the load, whereas the short time constant facilitates the cooling of the components, especially if they are exposed to wind. Figure 1 depicts a standard thermal model for an underground cable based on the stated contexts. The equivalent thermal circuit of the DN components can be modeled similarly to the underground cables illustrated in Figure 1. After determining the time constant of the components, the components' hourly rating can be computed using the following equations such that the hottest-spot temperature of each component should be less than its thermal limit (e.g., 90 °C).

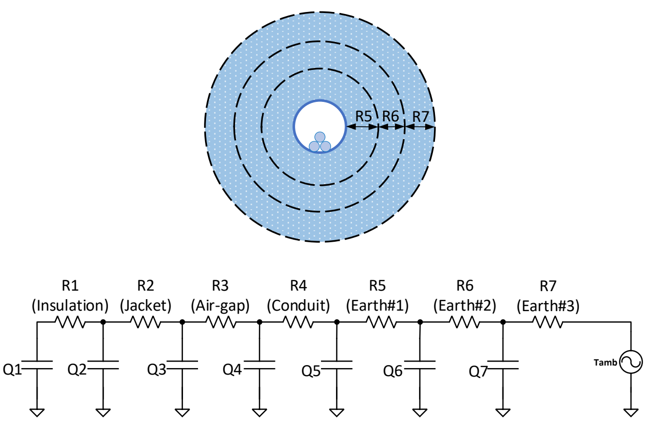

Figure 1. Standard electro-thermal model for an underground cable.

$$\theta_n(t_I) = \theta_{d,n} + \theta_{amb}(t_I) + \sum_m \theta_{n,m}(t_I) \quad (3)$$

$$\theta_{n,m}(t_I) = \theta_{n,m}(t_{I-1}) - T_{n,m}W_c(\theta_c(t_{I-1}))e^{-\frac{t_I - t_{I-1}}{\tau_k}} + T_{n,m}W_c(\theta_c(t_{I-1})) \quad (4)$$

In (3), $\theta_n(t_I)$ refers to the temperature of the node n between all nodes indicated in Figure 1 at time t_I. Moreover, $\theta_{d,m}$ represents the raised temperature arising from the dielectric losses in node n. Furthermore, θ_{amb} and $\theta_{n,m}$, respectively, indicate the ambient temperature and temperature difference among nodes n and k. The nodal time constant is also indicated with τ_m in the above formulation. In addition, the control parameter $T_{n,m}$ is used in (4) to control the exponential equations, in which subscripts n and k represent the considered node and the ladder circuit's thermal loop, respectively. Finally, $W_c(\theta_c(t_{I-1}))$ refers to the conductor loss in conductor temperature $\theta_c(t_{I-1})$ at time t_{I-1}.

Complicating the computation is the hourly rating of the DN's components as real-time DTR, performed by accessing the previous hour and initial state thermal conditions of these components and ecological states, e.g., ambient temperature, wind speed, and solar radiation. Thus, according to the real-time changes in the component's loading and environmental status, (1) and (2) are used to adjust the thermal resistances and thermal capacitance of conductors and components. IEEE standards 738 [27] and C57.91-2011 [28] are used to compute the next hour's updated ratings of the overhead lines and transformers based on the initial and previous hour thermal status and environmental conditions, including the ambient temperature, solar irradiation, and wind.

2.3. Objective Function

The distribution network operator seeks to manage the peak load in a way that minimum cost is incurred by applying the curtailment, and the lowest acceptable system indices are met. Consider a day that the network is in an overloading condition for the peak hour period of $\Omega_h = \{h_1, \ldots, h_n\}$, known as event hours. The total cost function Γ over this period and its relevant constraints are given in (5)–(10). It should be noted that the investment costs of equipment required for the proposed management methods, such as current transformers, thermometers, and smart grid infrastructure, have not been considered in the proposed operation optimization problem (5)–(10).

$$\Gamma = \sum_{h\in\Omega_h} \rho_h^G P_h^G + \sum_{h\in\Omega_h} \sum_{i'\in\Omega_c} \rho_{i',k(i')}^{cur} \chi_{i',h} P_{i',h}^0 \quad (5)$$

Subject to

$$P_h^G = \sum_{i\in\Omega_L} (1-\chi_{i,h})P_{i,h} + S_{base} \sum_{S\in\Omega_S} r_s I_{s,h}^2 \quad (6)$$

$$[\mathbf{V_h}, \mathbf{I_h}] = \mathbf{f}(\boldsymbol{\varnothing}, \mathbf{P_h^0}, \mathbf{Q_h^0}, \mathbf{Z}, V_h^{Sub}) \quad (7)$$

$$V^{\min} \le V_{i,h} \le V^{\max} \quad (8)$$

$$I_{s,h} \times I_{base} < I_s^R u_s(\theta, w, \varphi, h) I_h^{Tr} < I_s^{Tr,R} u_{Tr}(\theta, w, \varphi, h) \quad (9)$$

$$\chi_{i,h} \le MCL \quad (10)$$

In (5), ρ_h^G is the hourly market energy price, and P_h^G is the hourly purchased power from the upstream grid. In the primary power trading structures, distribution utilities had to sell the electricity to the customers by purchasing energy from utilities with a monopoly on the power delivery network. In contrast, in the restructured energy market, distribution companies participate in the wholesale market to buy energy and sell it to the customers (besides the retailers), which is reflected by the first term of the objective function (5). Set of Ω_L denotes the set of load points that participated in the curtailment program, $\rho_{i,k}^{cur}$ is the penalty price for every kW of load curtailment, considering the type of customers, e.g., residential or industrial. Variable $\chi_{i,h}$ determines the curtailment amount of each load, and $P_{i,h}^0$ is the hourly baseline load. Equation (6) states the hourly purchasing power is the sum of the CVR-effected loads with curtailment and total network loss. The variables Ω_L and Ω_S are, respectively, the set of load points and sections, S_{base} is base power, r_s is the per-unit section resistance, and $I_{s,h}$ is the per-unit current of sections. Function $f(.)$, gives the bus voltages and section currents through the power flow in substation voltage of V_h^{sub}. The vector **Z** is the impedance vector of the distribution network. Constraints (8) and (9) state the limitations on bus voltage, section current, and HV/MV transformer current I_h^{Tr}. Parameters $V^{\min}$, $V^{\max}$, and I_{base}, respectively, denote the voltage bounds and base current; $I_s^R$and $I_s^{Tr,R}$, respectively, stand for the rated current limits of feeders and HV/MV transformers. Both $u_s(\theta, w, \varphi, h)$ and $u_{Tr}(\theta, w, \varphi, h)$ are functions of temperature, wind speed, solar irradiation, and hour. Inequality (10) states that the curtailment amount is restricted within a maximum curtailment level (MCL) and must not exceed this value.

3. Soution Algorithm

According to the previous section, the noted peak management is a nonlinear problem with complex power flow constraints. Several meta-heuristic algorithms such as numerical methods can be used for combinatorial problems and optimization of models with high nonlinearity. Simulated Annealing (SA), artificial bee colony (ABC), and genetic algorithm (GA) are well-known heuristic methods. Notwithstanding the individual advantages of these algorithms, the introduced problem has a model with pure continuous variables. This is a unique characteristic that outweighs the particle swarm optimization algorithm (PSO) over other algorithms such as GA because it has an acceptable convergence. Hence, this paper proposes the PSO as a computational meta-heuristic method, which is appropriate for problems with all continuous variables [30].

Here, to solve our peak management problem, particle positions differ by operator strategy. For the no-CVR strategy, the generated solution goal is to find curtailment amounts, whereas in CVR and DTR strategies, the optimum substation per-unit voltage has to be found. The particle structure in the PSO to solve this problem for each event hour is shown in Figure 2.

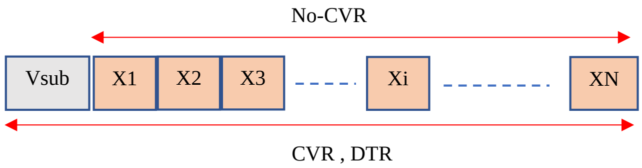

Figure 2. Structure of particles for each event hour.

The CVR problem uses power flow analysis to find the bus voltages and branch currents and to check any voltage current violation in the network. Because the loads experienced curtailment, linear power flow is not applicable, i.e., it becomes a complex nonlinear constraint. Thus, mathematical programming optimization models do not seem suitable for this problem, whereas heuristic optimization models can be so helpful in solving such issues. Backward–forward sweep (BFS) is used as the power flow algorithm in this manuscript. The BFS algorithm is a numerical method to solve the power flow of radial distribution feeders. Other numerical methods, such as Newton Raphson, are suitable for high-voltage meshed networks. AC power flow modeled within the mathematical programming framework over-complicates the solving procedure because it dramatically enhances the nonlinearity in the presence of demand response. The algorithm proposed here to solve the power flow is based on the bus injection branch current (BIBC) matrix Ψ, with a primary size of $N_S \times N_B$ [31]. This binary matrix gives the section currents of the network concerning the injected currents of the load points downstream of the section and has a form as below. Note that in the construction of the BIBC matrix, the first column has to be omitted to result in a square matrix.

$$\Psi = \begin{pmatrix} 0 & 1 & \cdots & 1 \\ 0 & 1 & \ddots & 0 \\ 0 & 0 & \cdots & 1 \end{pmatrix} \tag{11}$$

In order to find the BIBC matrix of a radial distribution network, a simple algorithm is introduced in [31]. Nevertheless, it necessitates a regular numbering of nodes and sections starting from the substation to the downstream nodes. Additionally, to cope with this drawback, a general algorithm is proposed in Algorithm 1, which leads to the construction of the BIBC matrix. In Algorithm 1, A is the adjacency matrix of the network by indicating that the substation nodes are all denoted by the number 1. The basis of Algorithm 1 is to find the leave nodes Ξ and their equivalent parent nodes s in the updated tree through the loop, as illustrated in Figure 3.

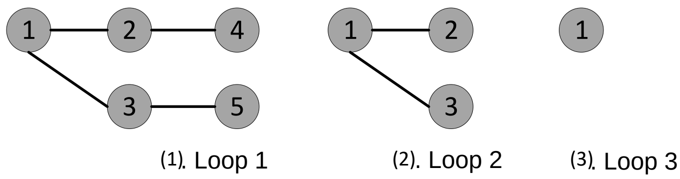

Figure 3. Updated tree of BIBC matrix.

Algorithm 1 Algorithm of BIBC matrix construction

Input: Matrix A representing network topology
Output: BIBC matrix *Initialization*:
Construct the adjacency matrix A
Create an empty cell array $\overrightarrow{\varphi}$ in length of network nodes
$f = N_S$
LOOP Process
while $(\Xi \neq \{\varnothing\})$ **do**
  $\Xi = \arg find(\sum_j A_{i,j} = 1)$
  for $(i = 1, i \leq |\Xi|)$ **do**
    $r = \Xi\{i\}$
    $\phi\{r\} = [\phi\{r\}, r]$
    $\Psi(n, \phi\{r\}) = 1$
    $s = \arg find(A(:, r) = 1)$
    $A(s, r) = 0, A = (r, s) = 0$
    $\phi\{s\} = [\phi\{s\}, \phi\{r\}]$
    $f = f - 1$
  end for
end while
return $BIBCMatrix$

For BIBC matrix construction, the backward–forward sweep can be implemented through the following algorithm (Algorithm 2). In this iterative algorithm, all the variables and parameters are considered as per-unit. To begin the algorithm, first, a diagonal matrix Z_D is constructed with elements equal to the impedance of sections as shown in (12). Next, a square matrix Y is constructed by Equation (13) to use in the algorithm. The bus voltages are calculated relative to the substation per-unit voltage V^{sub}. In each iteration, the same active and reactive power of the ZIP loads are obtained by functions g^P and g^Q described in (1) and (2). Note that curtailed powers of the load points must be considered in the power flow through the vector variable χ. Then, the current injection vector of each load is calculated using the Hadamard production ($\odot$). At the end of each iteration, bus voltages are updated by the equation in line 8 of the algorithm.

$$Z_D = \begin{pmatrix} z_1 & \cdots & 0 \\ \vdots & \ddots & \vdots \\ 0 & \cdots & z_N \end{pmatrix} \tag{12}$$

$$Y = \Psi^T . Z_D . \Psi \tag{13}$$

Figure 4 represents the entire flowchart for solving the problem of peak management for an overloaded distribution network. The optimal solution for each event hour is obtained, including the substation voltage and curtailment values. The generated solutions of PSO that violate the voltage and current limitations impose a penalty on the cost function.

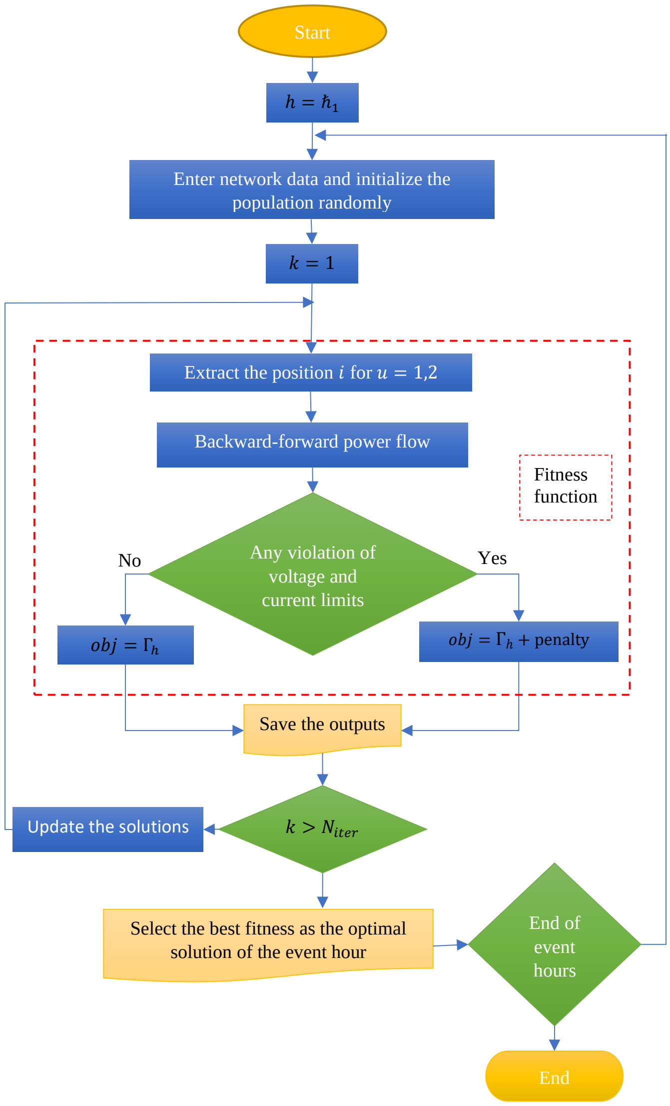

Figure 4. Solving algorithm of the problem.

Algorithm 2 Algorithm of backward–forward sweep

Input: BIBC matrix

Output: Results of power flow analysis (nodal voltage, branch current, loss) *Initialization*:

Construct the matrix Y

Create the vector of $V_0 = \overrightarrow{1} \times V^{sub}$ with length of number of load points and initiate the vector $\mathbf{V_B}$ as the bus voltages with $\mathbf{V_B} = \mathbf{V}_0$

$iter = 1$

LOOP Process

while $(iter \leq Maxiter)$ **do**

$\quad \mathbf{P} = g^P(\mathbf{V_B}, \mathbf{C_{z_p}}, \mathbf{C_{i_p}}, \mathbf{C_{p_p}}) \odot (1-\chi) \odot \mathbf{P^0}$

$\quad \mathbf{Q} = g^Q(\mathbf{V_B}, \mathbf{C_{z_q}}, \mathbf{C_{i_q}}, \mathbf{C_{p_q}}) \odot (1-\chi) \odot \mathbf{P^0}$

$$S = P + jQ, I = \left(s \odot \left[\frac{1}{V_B^1}, \frac{1}{V_B^2}, .., \frac{1}{V_B^N} \right]^T \right)^*$$

$\quad \mathbf{V}_B = \mathbf{V}_0 - \mathbf{YI}$

end while

return V, **I**

4. Simulation and Results

4.1. System under Study

The planned 144 bus Finnish DN is considered to study the main case studies of this paper in the overload condition. Figure 5 represents the single-line illustration of the system under investigation. The considered test system's annual peak load equals 11 MW. More details of the system under study, e.g., interruption costs, bus data, branch data, line size, and current rating, are given in [32]. As Figure 5 depicts, the 144 bus Finnish DN system consists of one primary 110/20 kV distribution substation that supplies 144 secondary 20/0.4 kV substations in a radial configuration. The ZIP model parameters used in this paper for load modeling are given in [33]. Furthermore, the weather-related data, e.g., ambient temperature, solar irradiation, and wind speed, are taken from [34]. The weather data related to the hottest day of the 2019 summer are used in the simulation process. The input data related to the hourly market prices and penalty costs are also given in [20,35]. Finally, the thermal specifications of the components, along with guides for simulating the thermal response of components, are derived from IEEE standards [27,29].

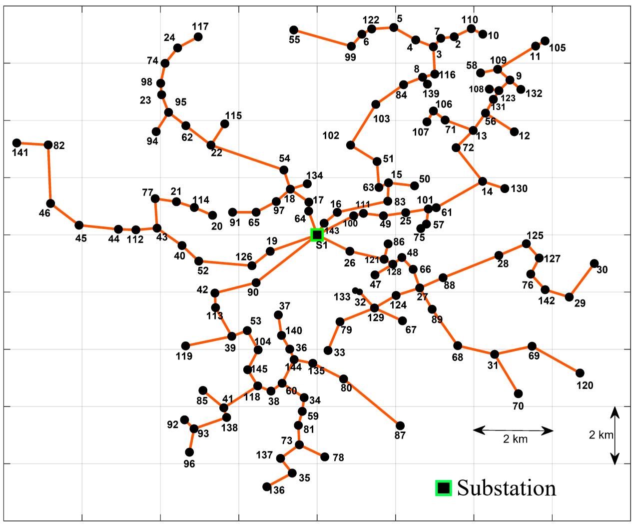

Figure 5. Single line representation of the test system under study.

4.2. Numerical Results

The obtained results are represented in three case studies, as listed below.

- Case 1: Operation of DN in normal mode without CVR and DTR;
- Case 2: Operation of DN with the implementation of CVR without considering DTR during the peak times (hour 10–hour 21);
- Case 3: Operation of DN with the implementation of CVR considering DTR during the peak times (hour 10 to hour 21).

Furthermore, the problems related to the increased line current with the implementation of CVR will be discussed.

4.2.1. Cost Results

The DN's operation costs show the main advantages of the proposed CVR-DTR incorporated with the DRP framework. As load curtailment is an expensive strategy, the operation cost of DN is reduced significantly in CVR and DTR strategies. In Figure 6a, the cost results of the introduced case studies are presented. According to Figure 6a, it can be shown that the DN's operation cost is $476,000, $293,000, and $51,400 during the peak hours (hour 10 to hour 21) for cases 1 to 3, respectively. From the noted results, it can be concluded that by the implementation of only the CVR, during the peak times, the system operation cost is reduced by 38.45%, whereas this cost reduction can be 89.2% with simultaneous implementation of DTR and CVR. In addition to the direct effects of the DTR in load curtailment reduction, which leads to peak cost reduction, the reason for lower cost reduction in case 2 compared to case 3 can be found in Figure 6b, so is critical to correctly interpret the results. According to Figure 6b, there appears to be a limitation that prevents more voltage reduction in case 2. This limitation is related to some buses containing significant constant-power loads. With more reduction of substation voltage, the substation transformer and branches carrying the current of these loads may experience more currents higher than their thermal current limits. Thus, the dynamic thermal rating of the substation transformer and branches allows more substation voltage reduction in case 3, which is illustrated in Figure 6b. According to the importance of this issue, more discussion is presented about current changes in what follows.

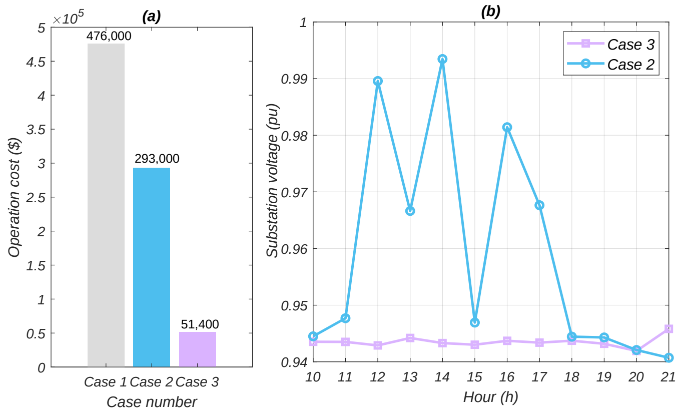

Figure 6. (**a**,**b**) Cost and voltage results of each case study.

4.2.2. Substation Power and Load Curtailment

In order to show the maximum use of the substation and line capacity in each case, the carried power from the 110/20 kV substation is illustrated in Figure 7. As noted, the use of DTR during the CVR implementation leads to a significant reduction in the cost due to more freedom in voltage reduction. This reduced cost level comes from the lower load curtailment in case 3 compared to case 2. In other words, the load curtailment during the events will be reduced by the implementation of DTR, and more loads will be supplied due to the increased thermal capacity of the DN components. This fact is illustrated in Figure 7. According to Figure 7, it can be concluded that by the dynamic thermal rating of the DN's components (branches and substation transformer in this paper), the supplied load through the substation is increased significantly in the third case compared to the second. The constant purchasing power from the market in case 2 is due to reaching the line capacity, which leads to curtailments of excessive loads. However, the capacity of feeders is increased in case 3 (with CVR), which increases the following energy and reduces the curtailed loads. In order to demonstrate the CVR and DTR effects in peak duration management clearly, the illustrative Figure 8 is presented to show the load curtailment in each case study. According to Figure 8, a slight reduction in curtailed loads happened in case 2 compared to case 1. Furthermore, a significant reduction is obtained due to the potential effects of the DTR in case 3, which is apparent in Figure 8.

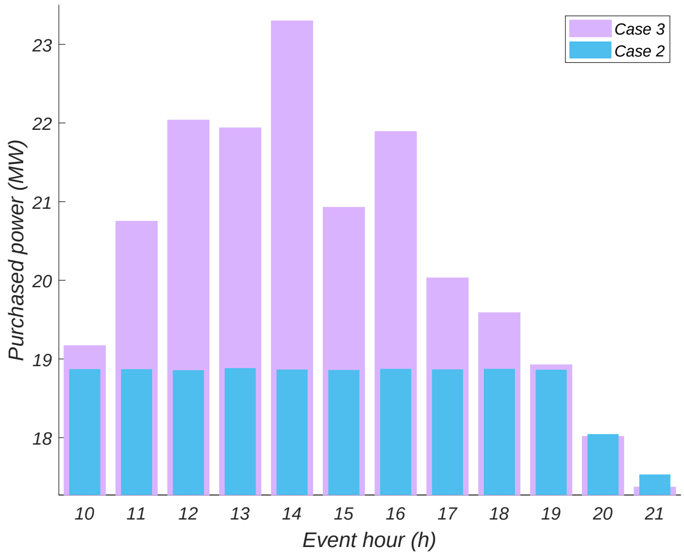

Figure 7. Carried power from the 110/20 kV substation during the event.

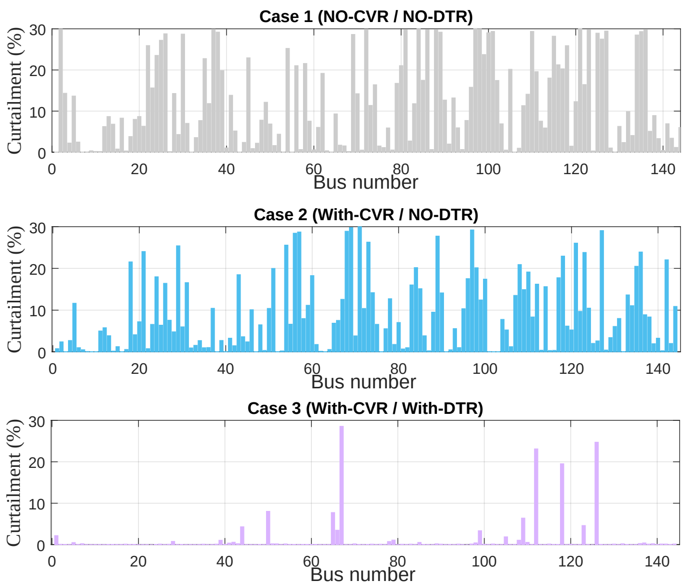

Figure 8. Curtailed loads of buses in each case study.

4.2.3. Voltage and Current Analysis

Figure 9 presents the bus voltage in each case studied for two event hours—10 and 14—that differ in temperatures, wind speed, and irradiation. According to Figure 9, the reduced voltage of case 2 compared to case 1 is evident by the implementation of CVR. The reduced voltage in both hours 10 and 14 are fairly close in cases 1 and 2, as illustrated in Figure 9. In contrast, in case 3, due to the difference in the local weather conditions (wind, solar, and temperature) of hours 10 and hour 14, more voltage reduction becomes possible in most buses. Furthermore, the branch current under case studies 2 and 3 is represented in Figure 10. From Figure 10, it is clear that in case 3, more currents are allowed to pass through the branches, especially in the near units to the substation, due to the potential effects of DTR.

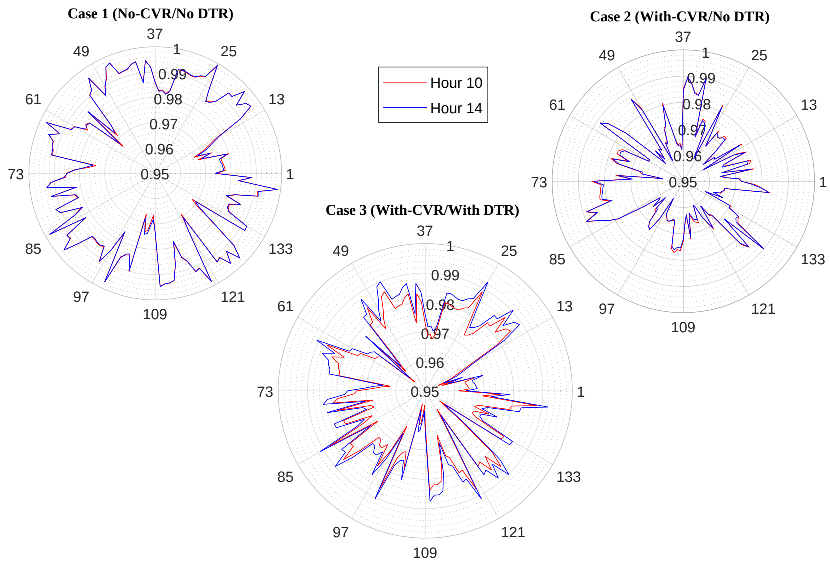

Figure 9. Buses voltages in each case study.

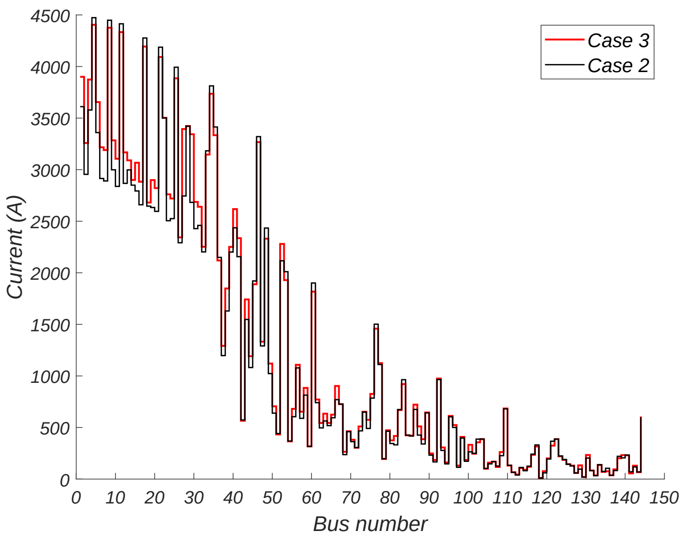

Figure 10. Branches current in each case study.

4.2.4. Effects of DN's Demand Factor on CVR Potential

As noted, due to the thermal limit of DN components, the CVR potential of DN depends on the loading condition of the whole network. Figure 11 shows the DN's potential for CVR under the different demand factors, which is interesting in analyzing the peak load management of DN using CVR. It is apparent in Figure 11 that the minimum voltage of DN is increased by raising the DN demand factor. A notable change in CVR potential happens in the demand factor of 95%, where the minimum CVR voltage is increased significantly. Thus, it can be concluded from Figure 11 that the CVR-based peak load management of DN may be considerably reduced by increasing the loading condition of DN.

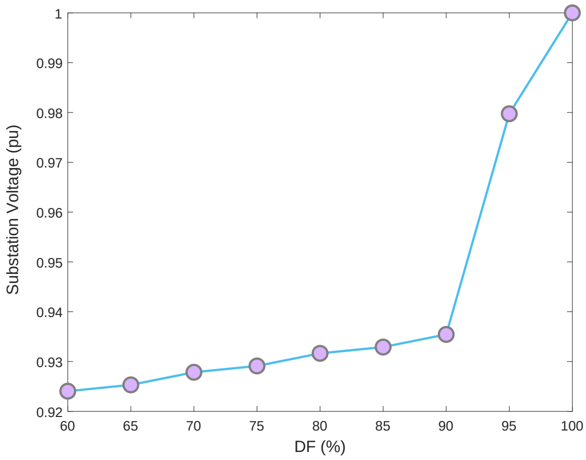

Figure 11. Effects of demand factor on CVR.

4.2.5. Current Changes of DN under CVR Considering the DTR

In order to clearly show the changes in currents of the feeders by CVR implementation, the graphical illustrative Figure 12 is used with the help of the color map. As is expected, there is more remarkable current change in the feeders nearest to the substation. Figure 12 highlights the beginning feeders with hot colors, which refer to the more significant changes in these feeders' currents. According to Figure 12, only some feeders experienced the high current changes that prevent CVR implementation.

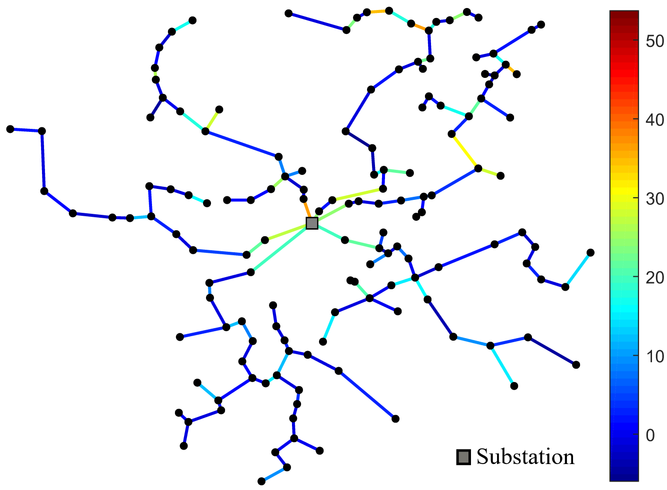

Figure 12. Current change in DN's feeders.

5. Discussion

In addition to the discussed advantages in system operation cost from implementing CVR and DTR, other impacts could be expected. Applying CVR by the operator has no significant effect on the lifetime of the network components. However, the loss can either increase or decrease in the sections of a feeder. Conducting CVR reduces the current consumption by the impedance loads, whereas the constant power loads face a current increase. Thus, we cannot give a definite expression about the impact of CVR on feeder losses. Unlike CVR, DTR implementation can reduce the feeder lifetime as it considers a short-time loading capacity higher than the nominal capacity for the cable. As well as CVR, DTR does not have a straightforward relationship with the feeder loss in this study. Moreover, It would be more efficient to apply the CVR to low voltage distribution networks, as the power management is conducted at the lowest level of the system. However, some essential points must be considered in this suggestion.

(1) Low voltage distribution feeders usually have a weak voltage profile, especially at the tail of the feeder, where the voltage is close to the lowest margin. Thus, reducing the substation voltage at the beginning of the feeder exposes the end-user customers to an undervoltage risk.
(2) Demand response implementation for load management requires an acceptable degree of automation. Therefore, CVR in this voltage level implies automatic demand response programs in practice and advanced distribution management systems.
(3) Low voltage distribution feeders are mainly penetrated by residential loads, limiting the CVR applicability.

The International Council for Large Electric Systems Working Group (CIGRE) recommended the DTR as a low-cost technology [36]. A techno-economic analysis of DTR during a long-term period is required to consider the added values of DTR (network expansion deferral, renewable energy integration, etc.) and imposed costs (equipment costs, impacts on life-cycle of components, etc.). The advantage of the DTR is dependent on the conditions of the network under study and weather conditions. Thus, an accurate justification for implementing DTR in the long term needs a long-term planning optimization problem, which could be considered interesting for future work.

6. Conclusions

This paper investigates three peak load management options of DN, including CVR, DTR, and DRP. CVR is widely discussed and introduced in previous literature, whereas less attention has been paid to DTR application in peak load management of DN. In addition to the direct effects of the DTR on peak load management of the DN, our investigations go beyond previous individual research, where the combination of the DTR into CVR leads to more advantages in the voltage reduction potential of the DN. Based on the reported results, the individual CVR leads to a 38.45% cost reduction during the peak hours, whereas the CVR considering DTR reduces cost by 89.2% for the same peak duration. Furthermore, the increased feeder's current by the implementation of CVR is proven in reported results, and DTR is investigated as a solution to this problem. Reducing load curtailment during peak events is an advantage of the proposed peak management framework. This reduction is considerable with simultaneous utilization of CVR and DTR. Based on the obtained results, the purchasing power from the electricity market is increased during peak times by utilization of CVR and DTR. It is worth noting that the load curtailment was considerable before CVR and DTR and is reduced using DTR and CVR as more loads are supplied. Despite several advantages, implementation of CVR and DTR requires a smart grid environment that limits the implementation of this approach in most conventional DNs.

Author Contributions: Investigation, K.Z.; Methodology, R.N., P.S. and B.M.-I.; Project administration, Z.A.-M.; Software, R.N.; Supervision, B.M.-I.; Validation, P.S., K.Z. and Z.A.-M.; Writing—original draft, R.N. and P.S.; Writing—review & editing, K.Z., B.M.-I. and Z.A.-M. All authors have read and agreed to the published version of the manuscript.

Funding: This research received no external funding.

Data Availability Statement: The dataset used and/or analyzed during the current study is availablefrom the corresponding authors on reasonable request.

Conflicts of Interest: The authors declare no conflict of interest.

Nomenclature

A. Indices

h	Index of time (hour)
i,j	Index of bus
s	Index of network sections
n,m	Index of node
B. Abbreviations	
DRP	Demand response program
CVR	Conservation voltage reduction
DTR	Dynamic thermal rating
DN	Distribution network
$BIBC$	Bus injection branch current
C. Parameters	
$P_{i,h}^0$	Active power of bus i before implementation of the CVR
$Q_{i,h}^0$	Reactive power of bus i before implementation of the CVR
$V_{i,h}^0$	Voltage of bus i before implementation of the CVR
C_{z_p}	Active power's Z coefficient of ZIP loads
C_{i_p}	Active power's I coefficient of ZIP loads
C_{p_p}	Active power's P coefficient of ZIP loads
C_{z_q}	Reactive power's Z coefficient of ZIP loads
C_{i_q}	Reactive power's I coefficient of ZIP loads
C_{p_q}	Reactive power's P coefficient of ZIP loads
$\theta_n(t_I)$	Temperature of the node n
θ_{amb}	Ambient temperature
$\theta_{n,m}$	Temperature difference among nodes
$\theta_{d,n}$	Temperature rise due to dielectric losses at node n
τ_n	Nodal time constant is also indicated
ρ_h^G	Hourly upstream market price
$\rho_{i,k}^{cur}$	Penalty price for every kW of load curtailment
$P_{i,h}^0$	Hourly baseline load
S_{base}	Base power
r_s	Per-unit section resistance
$\mathbf{Z}$	Impedance vector of the distribution network
$V^{\min}$	Minimum voltage limit of buses
$V^{\max}$	Maximum voltage limit of buses
I_{base}	Base current of sections
I_s^R	Rated current limits of feeders
$I_s^{Tr,R}$	Rated current limits HV/MV transformers
D. Variables	
$P_{i,h}$	Active power of bus i at time h
$Q_{i,h}$	Reactive power of bus i at time h
$V_{i,h}$	Voltage of bus i at time h
P_h^G	Hourly purchased power from the upstream grid
V_h^{sub}	Bus voltage
$I_{s,h}$	Per-unit current of sections
$\chi_{i,h}$	Curtailed amount of each load

References

1. Nourollahi, R.; Gholizadeh-Roshanagh, R.; Feizi-Aghakandi, H.; Zare, K.; Mohammadi-Ivatloo, B. Power Distribution Expansion Planning in the Presence of Wholesale Multimarkets. *IEEE Syst. J.* **2022**, 1–10. [CrossRef]
2. Evangelopoulos, V.A.; Georgilakis, P.S. Probabilistic spatial load forecasting for assessing the impact of electric load growth in power distribution networks. *Electr. Power Syst. Res.* **2022**, *207*, 107847. [CrossRef]
3. Dashti, R.; Afsharnia, S.; Ghasemi, H. A new long term load management model for asset governance of electrical distribution systems. *Appl. Energy* **2010**, *87*, 3661–3667. [CrossRef]
4. Darwazeh, D.; Duquette, J.; Gunay, B.; Wilton, I.; Shillinglaw, S. Review of peak load management strategies in commercial buildings. *Sustain. Cities Soc.* **2021**, *77*, 103493. [CrossRef]

5. Chakraborty, N.; Mondal, A.; Mondal, S. Efficient Scheduling of Nonpreemptive Appliances for Peak Load Optimization in Smart Grid. *IEEE Trans. Ind. Inform.* **2018**, *14*, 3447–3458. [CrossRef]
6. Fontenot, H.; Ayyagari, K.S.; Dong, B.; Gatsis, N.; Taha, A. Buildings-to-distribution-network integration for coordinated voltage regulation and building energy management via distributed resource flexibility. *Sustain. Cities Soc.* **2021**, *69*, 102832. [CrossRef]
7. Wang, Z.; Wang, J. Review on implementation and assessment of conservation voltage reduction. *IEEE Trans. Power Syst.* **2014**, *29*, 1306–1315. [CrossRef]
8. Warnock, V.J.; Kirkpatrick, T.L. Impact of voltage reduction on energy and demand: Phase II. *IEEE Trans. Power Syst.* **1986**, *1*, 92–95. [CrossRef]
9. Fletcher, R.H.; Saeed, A. Integrating engineering and economic analysis for conservation voltage reduction. In Proceedings of the IEEE Power Engineering Society Transmission and Distribution Conference, Chicago, IL, USA, 21–25 July 2002; Volume 2, pp. 725–730. [CrossRef]
10. Shukla, S.; Eldali, F.; Pinney, D. Cost-Benefit Analysis of Conservation Voltage Reduction Incorporated in Open Modeling Framework. In Proceedings of the IEEE Power and Energy Society General Meeting, Portland, OR, USA, 5–10 August 2018; Volume 2018. [CrossRef]
11. Mahendru, A.; Varma, R.K. Reduction in System Losses and Power Demand by Combination of Optimal Power Flow and Conservation Voltage Reduction Using Smart PV Inverters. In Proceedings of the IEEE Power and Energy Society General Meeting, Atlanta, GA, USA, 4–8 August 2019; Volume 2019. [CrossRef]
12. Faruqui, A.; Arritt, K.; Sergici, S. The impact of AMI-enabled conservation voltage reduction on energy consumption and peak demand. *Electr. J.* **2017**, *30*, 60–65. [CrossRef]
13. EL-Azab, M.; Omran, W.A.; Mekhamer, S.F.; Talaat, H.E. Congestion management of power systems by optimizing grid topology and using dynamic thermal rating. *Electr. Power Syst. Res.* **2021**, *199*, 107433. [CrossRef]
14. Huang, R.; Pilgrim, J.A.; Lewin, P.L.; Payne, D. Dynamic cable ratings for smarter grids. In Proceedings of the 2013 4th IEEE/PES Innovative Smart Grid Technologies Europe, ISGT Europe, Lyngby, Denmark, 6–9 October 2013. [CrossRef]
15. Pramayon, P.; Guerard, S.; Aanhaanen, G.; Kresimir, B.; Cachtpole, P.; Norton, M.; Puffer, R.; Sorensen, A.; Weibel, M.; Brennan, G.; et al. *Increasing Capacity of Overhead Transmission Lines Needs and Solutions*. TECHNICAL BROCHURES 2010. Available online: https://cigreindia.org/CIGRE%20Lib/Tech.%20Brochure/425%20Increasing%20capacigies%20of%20OHL%20TL.pdf (accessed on 5 August 2022).
16. Douglass, D.A.; Edris, A.A. Real-time monitoring and dynamic thermal rating of power transmission circuits. *IEEE Trans. Power Deliv.* **1996**, *11*, 1407–1415. [CrossRef]
17. Viafora, N.; Morozovska, K.; Kazmi, S.H.H.; Laneryd, T.; Hilber, P.; Holbøll, J. Day-ahead dispatch optimization with dynamic thermal rating of transformers and overhead lines. *Electr. Power Syst. Res.* **2019**, *171*, 194–208. [CrossRef]
18. Zhan, J.; Chung, C.Y.; Demeter, E. Time Series Modeling for Dynamic Thermal Rating of Overhead Lines. *IEEE Trans. Power Syst.* **2017**, *32*, 2172–2182. [CrossRef]
19. Palensky, P.; Dietrich, D. Demand Side Management: Demand Response, Intelligent Energy Systems, and Smart Loads. *IEEE Trans. Ind. Inform.* **2011**, *7*, 381–388. [CrossRef]
20. Nourollahi, R.; Salyani, P.; Zare, K.; Mohammadi-Ivatloo, B. Resiliency-oriented optimal scheduling of microgrids in the presence of demand response programs using a hybrid stochastic-robust optimization approach. *Int. J. Electr. Power Energy Syst.* **2021**, *128*, 106723. [CrossRef]
21. Yu, D.; Liu, H.; Bresser, C. Peak load management based on hybrid power generation and demand response. *Energy* **2018**, *163*, 969–985. [CrossRef]
22. Ul Hassan, N.; Khalid, Y.I.; Yuen, C.; Tushar, W. Customer engagement plans for peak load reduction in residential smart grids. *IEEE Trans. Smart Grid* **2015**, *6*, 3029–3041. [CrossRef]
23. Aalami, H.A.; Moghaddam, M.P.; Yousefi, G.R. Demand response modeling considering Interruptible/Curtailable loads and capacity market programs. *Appl. Energy* **2010**, *87*, 243–250. [CrossRef]
24. Hossan, M.S.; Chowdhury, B. Integrated CVR and Demand Response Framework for Advanced Distribution Management Systems. *IEEE Trans. Sustain. Energy* **2020**, *11*, 534–544. [CrossRef]
25. Safdarian, A.; Degefa, M.Z.; Fotuhi-Firuzabad, M.; Lehtonen, M. Benefits of Real-Time Monitoring to Distribution Systems: Dynamic Thermal Rating. *IEEE Trans. Smart Grid* **2015**, *6*, 2023–2031. [CrossRef]
26. Manbachi, M.; Farhangi, H.; Palizban, A.; Arzanpour, S. Quasi real-time ZIP load modeling for Conservation Voltage Reduction of smart distribution networks using disaggregated AMI data. *Sustain. Cities Soc.* **2015**, *19*, 1–10. [CrossRef]
27. *IEEE Std 738-2012 (Revision of IEEE Std 738-2006—Incorporates IEEE Std 738-2012 Cor 1-2013)*; IEEE Standard for Calculating the Current-Temperature Relationship of Bare Overhead Conductors. IEEE: Piscataway, NJ, USA, 2013; pp. 1–72. [CrossRef]
28. *IEEE Std C57.91-2011 (Revision of IEEE Std C57.91-1995)*; IEEE Guide for Loading Mineral-Oil-Immersed Transformers and Step-Voltage Regulators. IEEE: Piscataway, NJ, USA, 2012; pp. 1–123. [CrossRef]
29. Degefa, M.Z.; Lehtonen, M.; Millar, R.J. Comparison of air-gap thermal models for MV power cables inside unfilled conduit. *IEEE Trans. Power Deliv.* **2012**, *27*, 1662–1669. [CrossRef]
30. Hossain, M.A.; Pota, H.R.; Squartini, S.; Abdou, A.F. Modified PSO algorithm for real-time energy management in grid-connected microgrids. *Renew. Energy* **2019**, *136*, 746–757. [CrossRef]
31. Teng, J.H. A direct approach for distribution system load flow solutions. *IEEE Trans. Power Deliv.* **2003**, *18*, 882–887. [CrossRef]

32. Kazemi, S. Reliability Evaluation of Smart Distribution Grids. Ph.D. Thesis, School of Electrical Engineering, Aalto University, Espoo, Finland, 2011; p. 147.
33. Khalili, T.; Jafari, A.; Kalajahi, S.M.S.; Mohammadi-Ivatloo, B.; Bidram, A. Simultaneous Demand Response Program and Conservation Voltage Reduction for Optimal Operation of Distribution Systems. In Proceedings of the 2020 IEEE Industry Applications Society Annual Meeting, IAS 2020, Detroit, MI, USA, 10–16 October 2020; Institute of Electrical and Electronics Engineers Inc.: Piscataway, NJ, USA, 2020. [CrossRef]
34. Available online: https://en.ilmatieteenlaitos.fi/open-data-sets-available (accessed on 5 August 2022).
35. Nourollahi, R.; Salyani, P.; Zare, K.; Razzaghi, R. A two-stage hybrid robust-stochastic day-ahead scheduling of transactive microgrids considering the possibility of main grid disconnection. *Int. J. Electr. Power Energy Syst.* **2022**, *136*, 107701. [CrossRef]
36. Increasing Capacity of Overhead Transmission Lines: Needs and Solutions. Available online: https://e-cigre.org/publication/425-increasing-capacity-of-overhead-transmission-lines-needs-and-solutions (accessed on 21 March 2021).